Current Topics in Catalysis
Vol. 11, 2014

Original Communication

Reduction of carbon dioxide using a visible-light-induced electron transfer system with colloidal metal nanoparticle catalysts: Evidence for production of methane

Kazutaka Hirakawa[1,2,*], Yumi Yamaji[3], Tetsu Yonezawa[4] and Naoki Toshima[5]

[1]Department of Applied Chemistry and Biochemical Engineering, Graduate School of Engineering, Shizuoka University, Johoku 3-5-1, Naka-ku, Hamamatsu, Shizuoka 432-8561, Japan; [2]Department of Optoelectronics and Nanostructure Science, Graduate School of Science and Technology, Shizuoka University, Johoku 3-5-1, Naka-ku, Hamamatsu, Shizuoka 432-8561, Japan; [3]Department of Applied Chemistry, School of Engineering, The University of Tokyo, Hongo 7-3-1, Bunkyo-ku, Tokyo 113-8654, Japan; [4]Division of Materials Science and Engineering, Faculty of Engineering, Hokkaido University, Kita 8, Nishi 5, Kita-ku, Sapporo, Hokkaido 060-0808, Japan; [5]Department of Applied Chemistry, Faculty of Engineering, Tokyo University of Science Yamaguchi, Daigaku-dori 1-1-1, Sanyoonoda-shi, Yamaguchi 756-0884, Japan.

ABSTRACT

A visible-light-induced electron transfer system was constructed in aqueous solution to reduce carbon dioxide. The electron transfer system consisted of tris(2,2'-bipyridine)ruthenium(II) chloride, methyl viologen, ethylenediaminetetraacetic acid (EDTA, a sacrificial electron donor), and a colloidal metal nanoparticle as a catalyst. When the colloidal metal nanoparticle catalysts prepared by alcohol reduction of metal salts were used for this system, methane was generated by direct decomposition of the contained ethanol. Hence, the colloidal platinum and ruthenium nanoparticle catalysts protected by micelle and liposome were prepared by photoreduction of corresponding metal salts in aqueous media without ethanol and used for the electron transfer system to generate methane. The methane generation from carbon dioxide was confirmed by isotopic experiments using $NaH^{13}CO_3$ as a carbon dioxide source. In addition to methane-^{13}C, methane-^{12}C was also detected in this experiment. The methane-^{12}C is considered to be generated from carbon dioxide produced by the decomposition of EDTA. Micelle-protected ruthenium and liposome-protected platinum nanoparticle catalysts showed relatively high efficiency for methane generation from carbon dioxide in this study.

KEYWORDS: metal nanoparticle, carbon dioxide, methane, hydrogen, photoreduction

1. INTRODUCTION

Artificial photosynthesis is an important approach for the application of catalysis to solve the energy problem and to reduce carbon dioxide in the atmosphere [1-4]. Solar energy provides us with the source of mass-energy cycles. Visible-light energy from the sun is converted to chemical energy by photosynthesis by plants. It is yet impossible for human beings to construct a complete artificial photosynthetic system. However, a model system can be constructed by using visible light as an energy source. One of the most important themes of artificial photosynthesis is the visible-light-assisted reduction of carbon dioxide [2, 4-6]. A visible-light-induced electron transfer

*Corresponding author
hirakawa.kazutaka@shizuoka.ac.jp

system with a catalyst is a model reaction system for this purpose. In the case of a visible-light reaction, methane, an eight-electron reduction product of carbon dioxide (Figure 1), is a thermodynamically favorable product [4]. We reported hydrogen generation from water in the visible-light-induced electron transfer system of ethylenediaminetetraacetic acid (EDTA) disodium salt, tris(2,2'-bipyridine)ruthenium(II) dichloride ($[Ru(bpy)_3]Cl_2$), 1,1'-dimethyl-4,4'-bipyridinium dichloride (methyl viologen, MV), and a colloidal metal nanoparticle catalyst [7-9]. This system could be used for the reduction of carbon dioxide to produce methane by bubbling a carbon dioxide gas into the system (Figure 1). In a previous report, we confirmed the production of methane in this system [10]. However, it has not been confirmed whether the methane is the reduction product of carbon dioxide or whether it comes from other carbon resources such as ethanol and EDTA, which have been added to the system as a reductant of metal ions to prepare the colloidal metal nanoparticle catalyst and as an electron source in the visible-light-induced electron transfer system, respectively. In this paper, photoreduction of carbon dioxide is carried out in a similar system using nanoparticle catalysts prepared by a photoreduction method [11] without ethanol. The origin of carbon of the methane has been confirmed to be carbon dioxide by isotopic experiments.

2. MATERIALS AND METHODS

2.1. Materials

Metal salts, hexachloroplatinic(IV) acid ($H_2PtCl_6 \cdot 6H_2O$) and ruthenium(III) dichloride ($RuCl_3 \cdot 3H_2O$) and protective agents for colloidal dispersions of metal nanoparticles, poly(*N*-vinyl-2-pyrrolidone (PVP, K30, MW: 40,000), polyethyleneglycol monolaurate ($C_{12}EO$), and lecithin (beans) were purchased from Tokyo Chemical Industry Co., Ltd. (Tokyo, Japan). EDTA, MV, sodium hydrogencarbonate ($NaHCO_3$), and ethanol were from Wako Pure Chemical Industries Ltd. (Osaka, Japan). $[Ru(bpy)_3]Cl_2$ was prepared according to the literature [12].

2.2. Characterization of colloidal dispersion of metal nanoparticles

Colloidal dispersions of metal nanoparticles were characterized by transmission electron micrographs (TEMs) and UV-Vis absorption spectra measurements. TEMs of metal nanoparticles were taken using an H-7000 electron microscope (Hitachi, Tokyo, Japan) operated at 100 kV of acceleration voltage at a magnification of 200,000. The carbon-supported copper mesh microgrid was used as a support for the metal nanoparticles. The diameter of metal nanoparticles was measured on the basis of TEM photographs. The histogram of particle-size distribution and the average diameter were obtained on the basis of measurements of 300 particles in an arbitrary chosen area of the photograph. UV-Vis spectra were measured using a U-3900 spectrophotometer (Hitachi) to confirm the reduction of metal ions and characterize the colloidal dispersity.

2.3. Preparation of platinum nanoparticles by alcohol reduction

The colloidal dispersions of PVP-protected platinum nanoparticles were prepared by an alcohol reduction

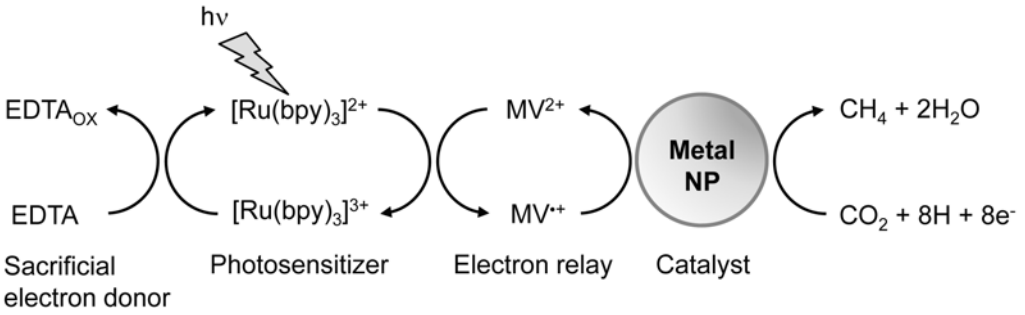

Figure 1. Schematic diagram of the visible-light-induced electron transfer system for the reduction of carbon dioxide by a metal nanoparticle catalyst. NP indicates nanoparticle.

method as previously reported [13]. 2.0 mmol PVP (40 times the mole of metal ions) and 0.050 mmol $H_2PtCl_6 \cdot 6H_2O$ were mixed in ethanol/water (1/1, v/v) to form a 50-cm^3 solution (concentration of metal ions: 1.0 mmol dm^{-3}). The mixed solutions were stirred and heated to refluxing at 95-100 ºC for 2 hours, giving brownish black colloidal dispersions. The average diameter of the platinum nanoparticles was 2.2 nm as per TEM measurement (described in the latter section).

2.4. Preparation of platinum and ruthenium nanoparticles by photoreduction

Colloidal dispersions of platinum and ruthenium nanoparticles were prepared by photoreduction of metal salts without using ethanol, according to the previous report [11]. Protective agents used for the metal nanoparticles were PVP, non-ionic surfactant ($C_{12}EO$), and liposome (LPS). A 50-cm^3 clean Pyrex Schlenk tube was filled with 10 cm^3 of an aqueous solution of protective agent and 10 cm^3 of an aqueous solution of $H_2PtCl_6 \cdot 6H_2O$ or $RuCl_3 \cdot 3H_2O$ (2.0 mmol dm^{-3}). The concentration of the protective agent (PVP or $C_{12}EO$) was 200 mmol dm^{-3}. An aqueous LPS solution was prepared as follows [14]: 40 mg of lecithin was dissolved in 2 cm^3 of chloroform in a 50-cm^3 flask; the chloroform was evaporated using a rotary evaporator to form a lecithin film inside the flask, and then the film was dissolved in 30 cm^3 of water by ultrasonication. The mixed solutions of the protective agent and the metal ion in water, degassed three times by freeze-thaw cycles and filled with nitrogen, were irradiated with an USHIO 500-W super-high-pressure mercury lamp (Ushio, Inc., Tokyo, Japan) for 2 hours with stirring, resulting in a brownish black colloidal dispersions. Production of platinum and ruthenium nanoparticles can be expressed by the following formulae:

$$H_2PtCl_6 + 2H_2O \rightarrow Pt + 2HClO + 4HCl \quad (1)$$

$$2RuCl_3 + 3H_2O \rightarrow 2Ru + 3HClO + 3HCl \quad (2)$$

UV-Vis spectra of these colloidal dispersions of metal nanoparticles are shown in Figure 2. Colloidal metal nanoparticle dispersions showed a specific shape of absorption spectra depending on the protective agent used. Figure 3 shows the TEMs of these metal nanoparticles. The average diameters of the metal nanoparticles, Pt-PVP, Pt-$C_{12}EO$, Pt-LPS, and Ru-$C_{12}EO$, were 1.6, 1.5, 1.4 and 1.5 nm, respectively.

2.5. Visible-light-induced reduction of carbon dioxide

Typical experiments were performed as follows: A 20-cm^3 Pyrex Schlenk tube was charged with an 8-cm^3 aqueous solution containing 125 mmol dm^{-3} EDTA, a sacrificial electron donor, 0.175 mmol dm^{-3} $[Ru(bpy)_3]Cl_2$, a photosensitizer, 1.75 mmol dm^{-3} MV, an electron relay, and 62.5 mmol dm^{-3} $NaHCO_3$, a pH adjuster. Two cm^3 of colloidal

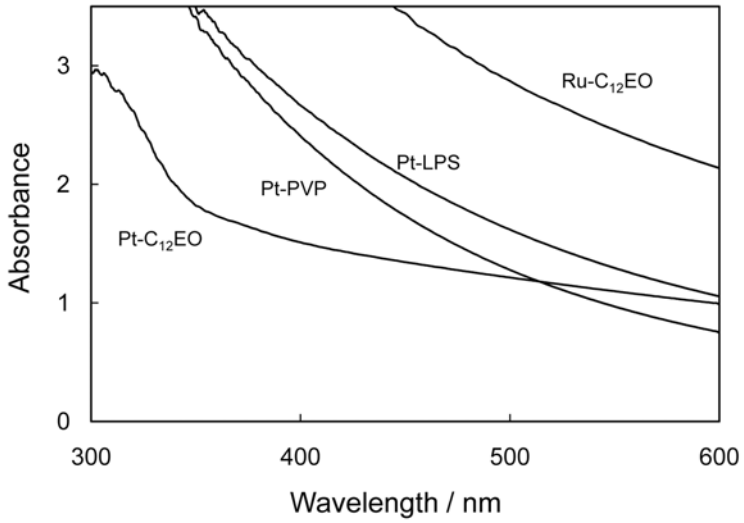

Figure 2. Absorption spectra of the colloidal dispersions of metal nanoparticles. [Metal] = 1.0 mmol dm^{-3}.

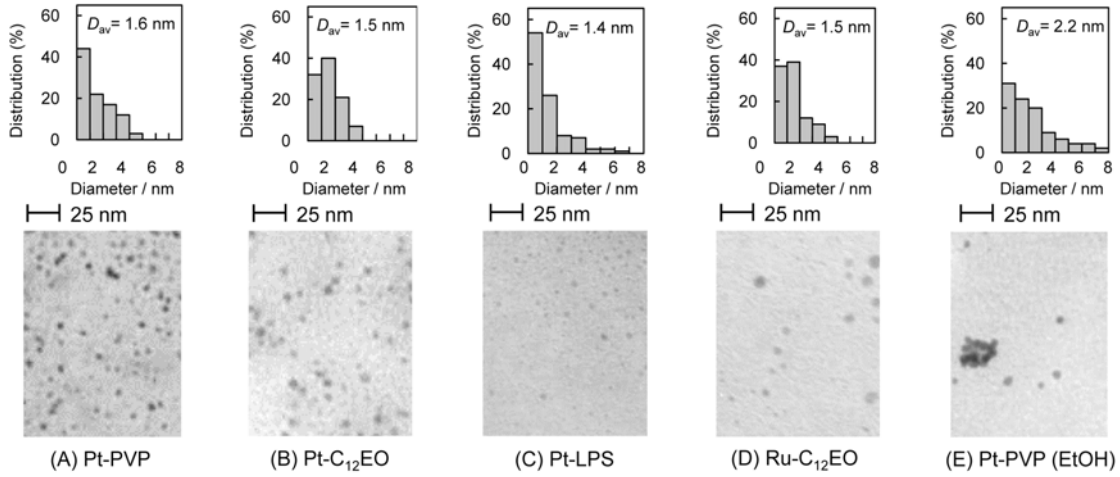

Figure 3. TEM micrographs and histograms of metal nanoparticles. D_{av} indicates the average diameter of metal nanoparticles. Metal nanoparticles were prepared by the photo-reduction (A to D) or the alcohol reduction (E).

dispersion of metal nanoparticles was added to the above solution. The mixtures were degassed three times by freeze-thaw cycles, and then the tubes were filled with 1 atm of carbon dioxide (Takachiho Chemical Industrial Co. Ltd., Tokyo Japan, purity: 99.95%). The photo-irradiation was carried out for 4 hours with an Ushio 500-W super-high-pressure mercury lamp through a UV cut filter (UV-39, Toshiba Co. (Tokyo Japan), > 390 nm) in a water bath maintained at 30 ºC.

2.6. Analysis of gaseous products

The products in the gas phase of the visible-light-induced reduction of carbon dioxide were analyzed with an Ohkura Riken (Saitama, Japan) model GC-103 (a Porapak Q column, at 60-120 ºC) and model GC-701 (an MS 13X column at 40 ºC) gas chromatograph. The yields were calculated with a System Instruments model 5000A intelligent integrator on the basis of the corresponding peak area. The characterization of gaseous products was carried out with a GC-14A gas chromatograph (Shimadzu, Kyoto, Japan) and a GC/MS-QP1100 EX gas chromatograph-mass spectrometer (GC-MS) (Shimadzu).

3. RESULTS AND DISCUSSION

3.1. Effect of contaminated ethanol on visible-light-induced methane generation

Methane generation was observed by visible-light irradiation applied to the electron transfer system composed of EDTA, $[Ru(bpy)_3]^{2+}$, MV, a colloidal metal nanoparticle catalyst, and CO_2, as reported earlier [10] (Figure 4). However, this system was contaminated with ethanol, which was used as a reductant for the preparation of colloidal metal nanoparticle catalysts with an alcohol reduction method. Thus, the possibility remains that the methane detected in this system originates not from carbon dioxide but from the contaminated ethanol. Therefore, an ethanol-free system was applied to visible-light-induced generation of methane from carbon dioxide. Since the original colloidal dispersions of metal nanoparticles prepared by alcohol reduction involved ethanol and water (1/1, v/v), all the solvents were removed from the dispersions by vacuum evaporation, and then the dried metal nanoparticles were again dispersed into the same amount of pure water as in the original dispersions. As a result, the amount of generated methane decreased in comparison with the original system containing ethanol. To this ethanol-removed system, the same amount of ethanol as that contained by the original system was added. Then nearly the same amounts of methane as in the original system were generated repeatedly, as shown in Figure 4.

The above experiment on the effect of ethanol on methane generation was carried out using ethanol-d5 instead of ethanol, and the amount of deuterium in the generated methane was measured with a GC-MS. In the results, five kinds of methane,

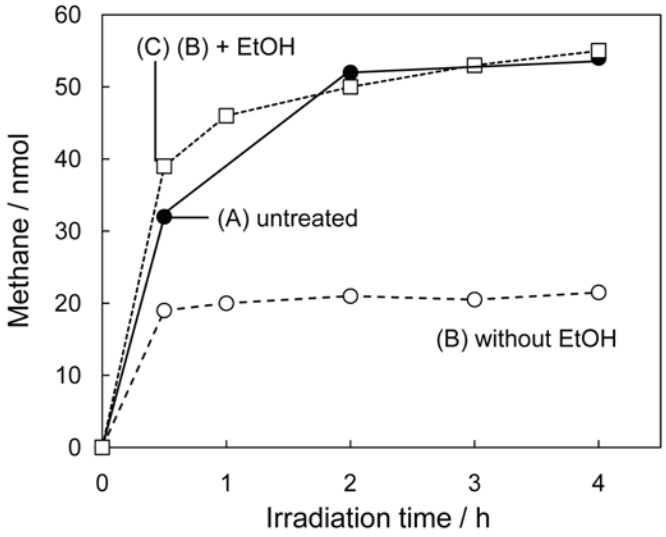

Figure 4. Effect of contaminated ethanol on the time course of methane generation under visible-light irradiation. Ten mL of aqueous solution containing 100 mmol dm^{-3} EDTA, 0.14 mmol dm^{-3} $[Ru(bpy)_3]^{2+}$, 1.4 mmol dm^{-3} MV, 0.20 mmol dm^{-3} (atomic concentration) Pt-PVP, and 50 mmol dm^{-3} $NaHCO_3$ was photo-irradiated (> 390 nm) under P_{CO_2} = 1 atm. (A) The system involving the Pt-PVP nanoparticle catalyst prepared by alcohol reduction (including 1 mL of ethanol in the system). (B) The ethanol-removed system involving the Pt-PVP nanoparticle catalyst prepared by alcohol reduction and the removal of ethanol under vacuum. (C) One mL of ethanol (the same amount as that of system (A)) was added to system (B).

CD_4, CD_3H, CD_2H_2, CDH_3, and CH_4, were detected by GC-MS, and the mole ratio of D to H in methane nearly equaled that calculated from the results shown in Figure 4. The methane generated in the ethanol-removed system is assumed to originate from carbon dioxide and that in the ethanol-containing system to originate from both carbon dioxide and ethanol. These results indicate that methane can be generated from ethanol when the system contains ethanol.

In the ethanol-containing system, methane could be generated not only by decomposition of ethanol but also by the reduction of carbon dioxide by ethanol. In order to confirm this possibility, $NaH^{13}CO_3$ was used as the source of carbon dioxide in the ethanol-containing system. The methane generated was not $^{13}CH_4$ but $^{12}CH_4$, indicating that methane was mainly generated by the decomposition of ethanol, not by reduction of carbon dioxide in the ethanol-containing system. Thus, the contaminated ethanol in the ethanol-removed system could have a large effect on the generation of methane by visible-light irradiation. The addition of methanol or 2-propanol to the ethanol-removed system slightly increased the methane generation as well (data not shown). These results suggest that in the present visible-light irradiation system, methane can be generated by the photoreduction of carbon dioxide, but it can be more easily generated by the decomposition of alcohols.

3.2. Evidence for photoreduction of carbon dioxide

As described in the previous section, contaminated ethanol can affect methane generation in the present system. Thus, complete removal of ethanol from the system is required to prove that the methane generation is by the photoreduction of carbon dioxide. However, it is very difficult to completely remove the contaminated ethanol from the colloidal dispersions of metal nanoparticles prepared by alcohol reduction. To avoid this problem, the colloidal dispersions of metal nanoparticles were prepared not by ethanol reduction but by photoreduction in water without ethanol. The photoreduction method also has the advantage of using micelle or LPS, which is stable in water and unstable in ethanol, instead of polymers as the protective colloid.

The photoreductions of platinum and ruthenium ions in the presence of micelle, LPS, or PVP were

carried out to produce colloidal dispersions of platinum and ruthenium nanoparticles. The electron transfer system involving CO_2 and the colloidal dispersions of platinum or ruthenium nanoparticles was irradiated with visible light. Then the formation of methane was clearly detected by gas chromatography (Figure 5).

In order to confirm the methane generation from carbon dioxide, isotope experiments were carried out using $NaH^{13}CO_3$ as the carbon source and a GC-MS analytical instrument. Since $NaHCO_3$ is equilibrated with CO_2 and NaOH in the solution, $NaHCO_3$ can generate CO_2, and CO_2 can be solidified with NaOH as $NaHCO_3$, which can be easily treated under atmospheric pressure in practical processes. Thus, $NaHCO_3$ is a good source of CO_2. The electron transfer system composed of EDTA, $[Ru(bpy)_3]^{2+}$, MV, a metal nanoparticle catalyst, and $NaH^{13}CO_3$ did produce methane under visible-light irradiation (Table 1). The produced methane was not completely $^{13}CH_4$ but contained $^{12}CH_4$ as well. The detected $^{12}CH_4$ is considered to originate from the organic materials contained in the electron transfer system. EDTA works as an electron donor in the system and is known to produce carbon dioxide as the final product. Thus, the effect of EDTA on $^{12}CH_4$ generation was examined in the Pt-LPS system. As shown in Table 1, the electron transfer system involving Pt-LPS and EDTA in the presence of $NaH^{13}CO_3$ did generate $^{13}CH_4$ and $^{12}CH_4$ at nearly the same mole ratio under visible-light irradiation. In this system, the mole ratio of $^{13}CO_2$ to $^{12}CO_2$ was almost 1:1, which is nearly the same as the isotopic ratio of the generated methane. These

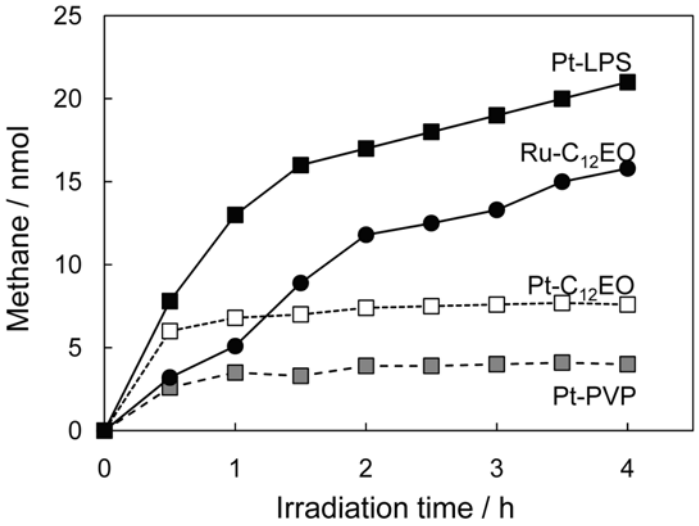

Figure 5. Time course of the visible-light-induced methane generation. Ten mL of aqueous solution containing 100 mmol dm^{-3} EDTA, 0.14 mmol dm^{-3} $[Ru(bpy)_3]^{2+}$, 1.4 mmol dm^{-3} MV, 0.20 mmol dm^{-3} (atomic concentration) metal nanoparticles prepared by photo-reduction, and 50 mmol dm^{-3} $NaHCO_3$ was photo-irradiated (> 390 nm) under P_{CO_2} = 1 atm.

Table 1. Methane generation and molar ratio of $^{13}CH_4$ and $^{12}CH_4$ in 3-hour irradiation.

Catalyst	**CH_4/nmol**	**$^{13}CH_4$ (%)**	**$^{12}CH_4$ (%)**
Pt-C_{12}EO	3.4	20	80
Ru-C_{12}EO	13	65	35
Pt-LPS	19	47	53

$NaH^{13}CO_3$ (50 mmol dm^{-3} in a 10 mL solution) was used as a carbon dioxide source.

results strongly suggest that the methane generated in this system originates from the photoreduction of carbon dioxide, which is from $Na^{13}HCO_3$ or decomposed EDTA.

3.3. Efficiency and selectivity of metal nanoparticle catalyst for photoreduction of carbon dioxide

Methane generation depends on the kind of metal nanoparticle catalysts (Figure 5). In addition, the isotopic experiments showed that the methane generation by photoreduction of carbon dioxide also depends on the protective agent (Table 1). The results showed that LPS is better than $C_{12}EO$ for photoreduction of CO_2. In addition, a comparison of the results of Pt-$C_{12}EO$ and Ru-$C_{12}EO$ reveals that ruthenium is better than platinum as a metal nanoparticle. Thus, Ru-LPS might be the best protected metal nanoparticle catalyst. We attempted to prepare the Ru-LPS in a similar way to the preparation of Pt-LPS, but the preparation of Ru-LPS was not successful. The resulting Ru-LPS was not as homogeneous, probably because $RuCl_3$ and LPS are not well miscible with each other in water. The suspension of Ru-LPS was not active as the catalyst for photochemical methane generation from carbon dioxide (data not shown).

In the present systems, hydrogen generation was more than hundreds of times the moles of methane generation (Figure 6). Therefore, the initial rate of hydrogen generation (r_{H_2}) almost indicates the total photoreaction rate (Table 2). The ratio of the initial rate of methane generation (r_{CH_4}) to the r_{H_2} should demonstrate the apparent selectivity of the

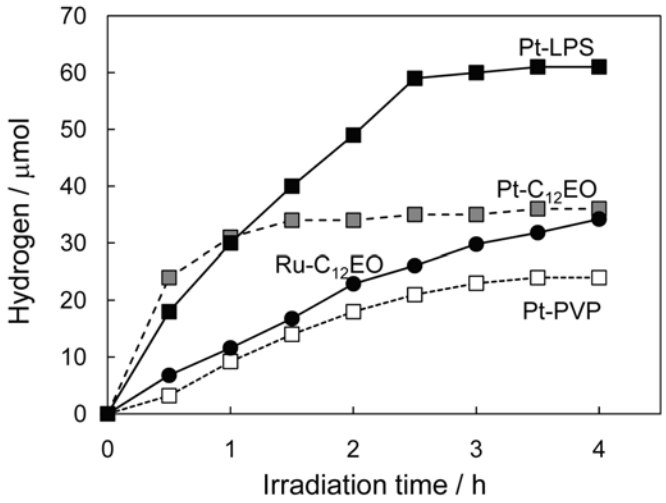

Figure 6. Time course of the visible-light-induced hydrogen generation. The experimental conditions are the same as in the caption of Figure 5.

Table 2. Methane and hydrogen generation rates.

Catalyst	r_{CH_4}/nmol min^{-1}	r_{H_2}/nmol min^{-1}	$r_{CH_4}/r_{H_2} \times 10^4$
Pt-PVP	0.20	110	18.2
Pt-$C_{12}EO$	0.09	800	2.9
Pt-LPS	0.26	600	3.3
Ru-$C_{12}EO$	0.11	230	4.8

r_{CH_4}: Initial rate of methane generation calculated from Figure 5.

r_{H_2}: Initial rate of hydrogen generation calculated from Figure 6.

r_{CH_4}/r_{H_2}: The relative selectivity of methane generation in the total reaction.

Table 3. Methane and hydrogen generation for 4-hour irradiation.

Catalyst	M_{CH_4}/nmol	M_{H_2}/μmol	$M_{CH_4}/M_{H_2} \times 10^4$
Pt-PVP	7.6	24	3.2
Pt-C_{12}EO	4.0	36	1.1
Pt-LPS	21.0	61	3.4
Ru-C_{12}EO	15.8	34	4.6

M_{CH_4}: Methane generation for 4 hours.
M_{H_2}: Hydrogen generation for 4 hours.
M_{CH_4}/M_{H_2}: The relative selectivity of methane generation for 4 hours.

methane generation in the total photoreaction. Estimated values suggested that Pt-PVP is an efficient catalyst for selective methane generation in terms of the initial reaction rate. However, the catalytic activity of Pt-PVP appeared to be deactivated within relatively short period. In terms of the absolute efficiency of methane formation, Pt-LPS and Ru-C_{12}EO showed high activity (Table 3). The activity of these catalysts continued for more than 4 hours.

4. CONCLUSION

Applying visible-light irradiation to the electron transfer system, composed of EDTA, $[Ru(bpy)_3]^{2+}$, MV, metal nanoparticle catalyst, and CO_2, generates a relatively large amount of hydrogen and a small amount of methane. The generated methane originates not only from the photoreduction of carbon dioxide but also from the decomposition of ethanol when the electron transfer system is contaminated by ethanol. Thus, platinum and ruthenium nanoparticle catalysts were prepared by a photoreduction method in water without ethanol. Using these metal nanoparticle catalysts, we successfully generated methane from carbon dioxide. The isotopic experiments using $NaH^{13}CO_3$ as a carbon dioxide source have proven that the generated methane originates from the photoreduction of carbon dioxide. Among the metal nanoparticle catalysts examined, Pt-LPS and Ru-C_{12}EO were found to be relatively active catalysts for photochemical methane generation from carbon dioxide. The efficiency and selectivity of the photoreduction of carbon dioxide to methane depend on the kind of metal, the size and dispersity of the metal nanoparticles, and the protective agents. Further investigations are required to develop a metal nanoparticle catalyst with high efficiency and selectivity for photochemical methane generation.

ACKNOWLEDGEMENTS

The present work is supported by a Grant-in-Aid for Scientific Research from the Ministry of Education, Culture, Sports, Science, and Technology of the Japanese Government.

CONFLICT OF INTEREST STATEMENT

The authors declare no competing financial interest.

ABBREVIATIONS

C_{12}EO, polyethyleneglycol monolaurate; EDTA, ethylenediaminetetraacetic acid disodium salt; LPS, liposome; MV, 1,1'-dimethyl-4,4'-bipyridinium dichloride; PVP, poly(*N*-vinyl-2-pyrrolidone; $[Ru(bpy)_3]Cl_2$, tris(2,2'-bipyridine)ruthenium(II) dichloride; TEM, transmission electron micrographs.

REFERENCES

1. Anpo, M. 2013, J. CO_2 Utilization, 1, 8.
2. Knör, G. Coord. Chem. Rev., in press. (doi:10.1016/j.ccr.2014.09.013).
3. Sato, S. and Ishitani, O. 2015, Coord. Chem. Rev., 282-283, 50.
4. Handoko, A. D., Li, K. and Tang, J. 2013, Curr. Opinion Chem. Eng., 2, 200.
5. Gui, M. M., Chai, S.-P. and Mohamed, A. R. 2014, Appl. Surface Sci., 319, 37.
6. Manzanares, M., Fàbrega, C., Ossó, J. O., Vega, L. F., Andreu, T. and Morante, J. R. 2014, Appl. Catal. B, 150-151, 57.

7. Toshima, N. and Hirakawa, K. 1997, Appl. Surface Sci., 121-122, 534.
8. Toshima, N. and Hirakawa, K. 1999, Polymer J., 31, 1127.
9. Hirakawa, K. and Toshima, N. 2003, Chem. Lett., 32, 78.
10. Toshima, N., Yamaji, Y., Teranishi, T. and Yonezawa, T. 1995, Z. Naturforsch., 50a, 283.
11. Toshima, N. and Takahashi, T. 1992, Bull. Chem. Soc. Jpn., 65, 400.
12. Palmer, R. A. and Piper, T. S. 1966, Inorg. Chem., 5, 864.
13. Hirai, H., Nakao, Y. and Toshima, N. 1979, J. Macromol. Sci. Chem., A13, 727.
14. Johnson, S. M., Bangham, A. D., Hill, M. W. and Korn, E. D. 1971, Biochim. Biophys. Acta, 233, 820.